

# Wireless, acoustically linked, undersea, magnetometer sensor network

Mihajlo Tomic, Peter T. Sullivan, and Vincent K. McDonald  
SSC-PACIFIC, 53560 Hull Street, San Diego, CA 92152  
mihajlo.tomic@navy.mil, sullivap@spawar.navy.mil, keyko.mcdonald.navy.mil

**Abstract**—This paper presents a magnetometer sensor node design that consists of a He3 nuclear precession total-field magnetometer, data acquisition and recording electronics, and acoustic modem for networking such nodes. Expounding, we describe the integration of an ultra-sensitive magnetometer with the support electronics just mentioned. Additionally, the fully integrated, stand-alone magnetometer sensor node's self-noise performance is presented and compared with reference magnetometers.

Due to the induced noise of the earth's background field, magnetometer data from multiple sensors is required in order to maximize the system detection range, thereby minimizing the overall number of required nodes to cover a given area. Given the aversion to continuously streaming data via the acoustic communications network between pairs of sensors, an alternative method is presented to minimize this traffic while still detecting objects of interest in the presence of the earth's field, with the cost being decreased detection ranges. Preliminary filtering techniques and an autoregressive process for implementing a noise whitening filter in addition to the application of orthonormal basis functions based on Anderson functions increase the single sensor detection range in the 0.001 to 0.030 Hz band representative of a passing vessel relative to the stationary sensor. The filter's noise suppression performance conducted onboard a single sensor and application to collected data is presented.

## I. INTRODUCTION

Advances in stationary, undersea, and passive total-field magnetic sensor technology allows for reduced size, power efficient, autonomous, passive surveillance capabilities for detecting, classifying, and tracking surface or submerged targets of interest. Traditional systems such as DADS (Deployable Autonomous Distributed System) have integrated these sensors on a common wired backbone with other sensing modalities, (i.e. acoustic, depth, heading, etc.). However, there are many advantages in developing wirelessly linked standalone magnetic sensing nodes using undersea acoustic communication modems for node-to-node collaboration. Because the magnetic sensor's output bandwidth is often less than 0.1 Hz for objects of interest to the US Navy, networking a wireless distributed field of these standalone sensors with acoustic communications is well within the limited undersea bandwidth. Nevertheless, minimizing communications between collaborating magnetometer sensor nodes is crucial to maintain a minimal presence and for sensor field persistence.

To support a networked undersea magnetometer sensor concept, the Polatomic Inc. He3 magnetometer and Teledyne/Benthos ATM-885 modem integration is critical. Initial integration efforts of a modem-to-magnetometer with  $pT/\sqrt{\text{Hz}}$  noise response in the milli-Hertz band (mHz) have

shown induced effects that reduce all functionality of the magnetic sensor. Subsequent integration efforts reduce these induced sources to immeasurable levels within the desired detection band of a passing vessel's magnetic signature and do not inhibit the performance of this ultra-sensitive magnetometer.

However, an undersea sensor network cannot support continuous data streaming between nodes. In order to limit underwater communication activity between nodes in the sensor field, initial detection is limited to a single magnetometer. Magnetic data processing must reduce the low frequency diurnal variation of the earth's magnetic field and employ a detection algorithm more effective than the standard energy detector. For this purpose, a single sensor detector first uses a whitening filter followed by the three orthonormal Anderson functions as individual matched filters.

## II. MODEM TO MAGNETOMETER INTEGRATION

Initial modem-to-magnetometer integration attempts led to significant degradation of sensor performance due to the shared ground plane of a common array. The preliminary integration of He3 magnetometer to DADS system employed separate batteries for the magnetometers and auxiliary sensors for the system; but a common ground plane was shared. The results, displayed in Figure 1, show high noise throughout the bandwidth of the magnetometer, approximately 85 dB greater than the noise floor of the He3 magnetometer in the mHz band. The gradiometer data shown in Figure 1 is generated by a time series subtraction of two pairs of magnetometers, one sensor on the array with coupled ground plane, and one sensor pair not connected to either a wired array or to one another.

These results influenced design of an integrated magnetometer - modem system. Just as in the previous testing, the magnetometer power supply was separated from the acoustic modem's. The utilization of independent batteries for power supply ensured some mitigation of electrically coupled noise from the high voltage required of the modem transducer during periods of communication. Having tested the common ground for a long wired array system, a common ground for the compact magnetometer - modem node was also attempted. Preliminary land based results showed no induced noise, and a sea test was conducted to verify these findings. Three different modem transmit source levels, each with two different message sizes, 28 and 1500 bytes, were tested. The results, Table I and Figure 2, show that although noise is present during bursts of

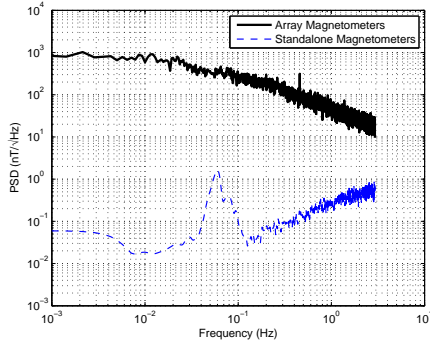


Fig. 1. Comparison of ground coupled and uncoupled gradiometer power spectral density for a wired array system.

TABLE I  
MODEM INTERFERENCE DURATION (SECS)

28 Byte Message			
	Power=4	Power=5	Power=6
MOD30	-	-	6
MOD31	-	-	13
MOD32	5	12	9
1500 Byte Message			
MOD30	-	-	38
MOD31	-	-	15
MOD32	27	28	15

acoustic communication, the interference does not approach the initial DADS system measured levels.

A final test was conducted to verify whether radiated magnetic interference induced by the modem transmission is present on the magnetometer. Local magnetic field perturbations can occur during these events, inducing noise on the magnetic sensor. A standalone modem, emitting messages of various lengths was placed within a meter of an independently operating magnetometer with complete electrical decoupling of the two devices. With no resulting interference present on the magnetometer due to modem transmission, the measurements show no interfering magnetic field associated with the acoustic communication transmission.

Thus, in the event that modem interference is present, it occurs to levels shown in Figure 2, and is due to the shared ground of the system. We will show that these levels do not inhibit the performance of a single sensor detector.

### III. DATA PROCESSING

Target signal response, modeled as a dipole, on the order of a few nano-Tesla (nT), compared to a background field exceeding 45,000 nT in mid latitudes, can be problematic to detect with only a single total-field magnetometer. Background noise suppression is required to improve signal to noise. Thus, certain assumptions are made in order to maximize the detection capabilities of a single magnetometer.

Velocity to slant range values,  $v/d$ , for a transiting vessel, determine the detection frequency band [1]. Considering only plausible  $v/d$  values, the bandwidth of interest is fully

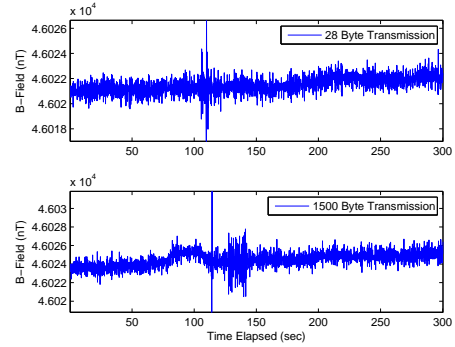


Fig. 2. Short and long acoustic modem transmission time response. Note the presence of high noise at 100 seconds (top plot) and 110 seconds (bottom plot).

captured in frequencies less than 30 mHz. With application of a bandpass filter, removal of the DC component of the geomagnetic field, and suppression of frequencies greater than 30 mHz, all residual noise from modem transmission is removed.

#### A. Whitening filter

Geomagnetic spectral structure is well documented with the conclusion that noise in the detection band of interest is non-white [3]. The application of a matched filter which results in an increase in single sensor detection range first requires He3 magnetometer data whitening, but only in the target detection band. To generate the whitened sequence, the He3 data is first bandpass filtered, which results in the removal of the DC component of the earth's background field, as well as the reduction of the higher frequency He3 sensor electronic noise present above 200 mHz. By band limiting and downsampling the data by a rate of 146 to 1 (from an original sampling frequency of 5.86 Hz), the whitening filter now only applies to the detection band, with remaining frequencies absolved from filter construction. By applying a forward linear predictor filter [4] of 20th order to a known *noise only* sequence of the data, spectrally white data is constructed.

$$\begin{aligned}
 r(n) &= \sum_{k=1}^{20} a_k r(n-k) + \nu(n) \\
 \hat{r}(n) &= \sum_{k=1}^{20} a_k r(n-k) \\
 \nu(n) &= r(n) - \hat{r}(n)
 \end{aligned}$$

The solution of the  $a_k$  coefficients is discussed in [3]. The difference between original and linear prediction filter results in a spectrally white sequence,  $\nu(n)$ , thus the flat structure in the mHz band shown in Figure 3.

#### B. Test case

Assuming constant course, speed, and depth relative to the stationary sensor, the magnetic sensor's signal response to a ferrous object is assumed to be a dipole moving through the

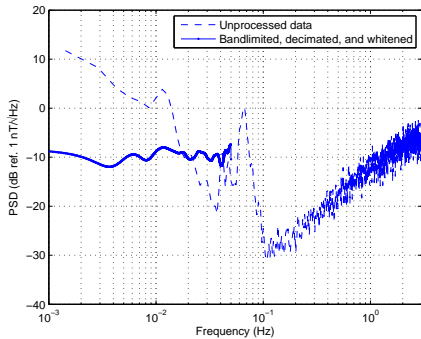


Fig. 3. Magnetometer data in the 1 to 30 mHz shows spectrally flat structure after the application of the whitening filter.

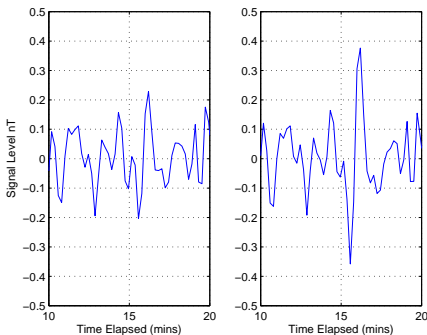


Fig. 4. The application of the Anderson matched filter to a noise only sequence (left) and one containing a magnetic signature (right) with the same  $v/d$  as the matched filter. The target is present at approximately 15 minutes in to the data set, and contains approximately 2 dB more SNR than the noise only case.

earth’s magnetic field. The Anderson functions [1] characterize the motion of this dipole with three orthogonal functions and are shown in Figure 5. The functions are dependent on a passing vessel’s target velocity to slant range ratio and time. This dimensionless parameter,  $vt/d$ , determine the period of the functions.

The Anderson functions, once properly normalized, [2] and [3], followed by the application of the same filtering and whitening applied to the He3 data sequence, are used individually as the matched filters for the single magnetometer detector [5]. Results of the detector in the presence of noise and the passing of a surrogate target created to resemble the research vessel R/V SPROUL, (approximately 40 m in length and magnetic moment of  $10^5 \text{ Am}^2$ ) compared to only the whitened signature data, are shown in Figure 4. Data processing from the results in Figure 4, show an estimated SNR gain of 2 dB when the target is present in the processing window. The data used to generate the whitening filter are extracted from the noise data set before the synthetic target signature is embedded on the data. Although a fixed  $v/d$  ratio is used, no target course is assumed and each individual basis function is used as a matched filter for each sequence of data. The process shows an approximate single sensor detection

slant range of 300 m for this synthetic target. This is an increase of 50% over a single sensor energy detector with the ability to only detect targets with  $\text{SNR} > 0 \text{ dB}$ .

### C. Undersea magnetometer network

Presently, the assumptions use an ideal choice of  $v/d$ , whitening filter coefficients created from a known sequence of magnetic noise, yet a low SNR is still achieved with the application of a matched filter. However, additional information provided by a neighboring sensor can further confirm the presence of a passing vessel after an initial single sensor detection has been met. This ability is conducted by requesting data from another sensor in the network, initiating the first exchange of information between sensors. Because the acoustic communications are limited and infrequent, this forces a single sensor detector to be as effective as possible.

The acoustic modem integration allows for the exchange of brief messages between sensors in the network, with the current implementation allowing for a data packet of 1500 bytes to be shared among the nodes. The current 146 to 1 downsample rate allows for one modem burst (less than 38 seconds in duration, Table I), to contain nearly two hours of magnetic data. Once initial detection has been made by a single sensor node without sensor-to-sensor communication, a second-stage process begins whereby pairs or groups of sensors share data over the acoustic link to verify the presence of a magnetic anomaly. Therefore, the low SNR shown in Figure 4 is not the final target detection determinant. Instead, the preliminary single sensor detection triggers sensor collaboration with the ability to exchange long durations of data in a short time period. With multiple sensor data now available, coherent subtraction of the background geomagnetic field can be conducted in order to verify the presence of a magnetic target.

Future work will address geomagnetic field reduction as well as the time delay cost for implementing such a system. Additionally, development of a prototype system is underway and is intended to verify these preliminary results. Real-time implementation and the use of inter-node data exchange for the tracking of passing targets is forthcoming.

## IV. CONCLUSION

Integration of a commercially available acoustic modem with an ultra-sensitive Polatomic He3 magnetometer show noise is dependent on the length of acoustic message sent. The efforts show that this modem induced magnetic noise is coupled through the common ground plane shared by the magnetometer and modem. The noise is outside the detection band of a vessel passing by the stationary sensor and does not inhibit the magnetometer’s detection capabilities.

The confined 30 mHz detection band requires bandpass filter application to reduce the geomagnetic effects while also suppressing the sensor electronics noise. The original  $1/f$  background noise is whitened. The orthonormal Anderson basis functions are passed through the same pre-processing methods. Using the processed Anderson functions as matched

